

# Thermal Expansion of Structure-H Clathrate Hydrates\*

JOHN S. TSE

Division of Chemistry, National Research Council of Canada, Ottawa, Ontario, Canada K1A 0R9

(Received: 9 April 1988; in final form: 24 June 1988)

**Abstract.** The temperature dependence of the unit cell parameters of two newly identified hexagonal structure clathrate hydrates of hexamethylethane (HME) and 2,2-dimethylbutane (DMB) have been measured by X-ray powder diffraction. The thermal expansion of the two distinct crystallographic axes was found to be inequivalent. However, the coefficients of cubic expansion are comparable to that in the cubic structure I and II hydrates. The larger thermal expansivity in the clathrate hydrates relative to ice is attributed to the weakening of the host lattice due to the internal pressure generated by the rattling motions of the encaged guests.

**Key words.** Clathrate hydrate, X-ray powder diffraction, thermal expansion.

## 1. Introduction

For a long time only two types of gas hydrates with cubic structures had been observed [1, 2]. Small molecules and rare gas atoms with molecular dimension less than 5.5 Å which can fit comfortably into the smaller cavities will form the type I structure [3, 4]. Molecules with dimension greater than 5.5 Å will favour the type II structure which has larger cages [5]. Up to 1986, no hydrate had been reported for a guest molecule with molecular size larger than 7 Å. Recent theoretical [6] and experimental [7] studies, however, show that very small guests, such as argon [7], krypton [7], oxygen [8] and nitrogen [9], form hydrates with the type II structure. It appears that the delicate balance between the weak intermolecular interactions between water and the guest and the *inherent* stability of the host lattice are the primary factors governing the structural preference [10]. More recently we reported [11] the preparation and characterization of a new type of clathrate hydrate (structure H) which is formed with organic molecules too large to fit into the cavities of the more familiar cubic type I and II structures.

Although there is no single crystal structure available for the new hydrate, X-ray and neutron powder diffraction patterns [11] show that the structure is isomorphous with the hexagonal clathrasil dodecasil-1H [12]. Thus it is reasonable to assume that the water framework of the hydrate is also composed of three different kinds of cages [12]. There are two small cages, a pentagonal dodecahedral  $5^{12}$  cage, which is common to many hydrate structures [1, 2], and a non-spherical 12-sided cage, also a dodecahedron, containing 4-, 5- and 6-sided polygons and designated as  $4^35^66^3$ . The most remarkable feature of the new structure is the presence of a large non-spherical cavity having 12 5-sided and 8 6-sided faces ( $5^{12}6^8$ ) where the large organic molecule resides.

\* Dedicated to Dr D. W. Davidson in honor of his great contributions to the sciences of inclusion phenomena.

The conditions for the formation of the structure H hydrates are relatively undemanding. It can be prepared by condensing the appropriate organic molecules onto powdered ice in the presence of a help gases such as hydrogen sulphide and xenon. In view of the ease of hydrate formation, it is highly likely that the structure H hydrate may occur naturally; in particular, in areas rich in hydrocarbons and hydrogen sulphide, such as in the gas and oil fields [13]. Therefore, it is of practical importance to study the stability and thermophysical properties of the structure H hydrate. In this paper, we report some preliminary results on the measurements of the thermal expansion of two structure H hydrates in the temperature range 80 to 230 K. The outline of this paper is as follows. In the next section we give details of the experimental procedure and the method of data analysis. The thermal expansion data will then be discussed and compared with the results obtained for other clathrate hydrates in section 3. We conclude this paper with a brief summary.

## 2. Experimental Section

### 2.1. HYDRATE PREPARATION

Structure H hydrates of hexamethylethane (HME) and 2,2-dimethylbutane (DMB) were prepared by sealing an appropriate amount of the solid (HME) or liquid (DME) in powdered ice in a glass tube containing a small amount of hydrogen sulphide and xenon at liquid nitrogen temperature. The sample tubes were then warmed and kept at dry ice temperature for about half an hour and then warmed and kept in an ice bath for several hours.  $^{129}\text{Xe}$  NMR was used to characterize the samples [11] from which it is apparent that for both hydrates the xenon was contained as structure H hydrate within 1 or 2 hours of preparation. The samples were later stored for several months at  $-30^\circ\text{C}$  before the X-ray experiments were performed.

It is very difficult to measure the stoichiometry of a four-component system and no such information is available for the structure H hydrate samples. In order to achieve maximum stability, the large cavities of the hydrate is likely to be fully occupied by the organic molecules and the xenon and hydrogen sulphide will occupy the smaller cages. In principle, gas hydrates are nonstoichiometric crystalline solids; however, the range of compositions in the stability region of hydrate formation is quite narrow under normal temperature and pressure conditions [14, 15]. For instance, for the structure I hydrate of ethylene oxide (EO), the equilibrium compositions can only vary between  $\text{EO} \cdot (6.76-7.21) \pm 0.07 \text{ H}_2\text{O}$  regardless of the concentration of the solution in which the hydrates were prepared [14]. Moreover, there is no strong evidence suggesting that the cell parameters of hydrates are dependent on the stoichiometry [16, 17].

### 2.2. X-RAY POWDER DIFFRACTION

The unit cell parameters of the hydrates were determined from their powder diffraction patterns. X-ray powder diffraction patterns were obtained with  $\text{CuK}_\alpha$  radiation using a Rigaku  $\theta-\theta$  wide angle diffractometer equipped with a nitrogen-jet cooled Anton-Parr low temperature camera and a graphite monochromator

situated in the diffracted beam. The diffractometer and the temperature controller have been calibrated against the thermal expansion of silicon powder and the *cubic*  $\rightarrow$  *monoclinic* phase transition of adamantane. In order to minimize water condensation and hydrate decomposition, the specimens were transported and mounted onto the goniometer at liquid nitrogen temperature. For each hydrate, a diffraction pattern from 5–55°  $2\theta$  was recorded. The diffraction pattern for HME hydrate is shown in Figure 1. Apart from a very small ice contamination, the diffraction peaks can be indexed according to a hexagonal space group with Laue symmetry of *6/mmm*. Although it would be preferable to obtain a full diffraction pattern at each temperature, it is a rather time consuming process and is impractical to do. Instead, the diffraction pattern of a small region from 28–32° was monitored as a function of the temperature. This angular region was chosen because it is completely free of ice contamination and the intensities of the diffraction peaks are strong enough to provide good statistics. The scan speed was 0.12°/min with an incremental step size of 0.004°. The typical count rate on a peak was about 100–200 cps. The raw data were smoothed using a spline fitting procedure [18] and the contributions from the  $\text{Cu}K_{\alpha 2}$  radiation were eliminated according to the modified Rachinger method [19, 20].

The diffraction patterns for the HME and DME hydrate in the 28–32° region are shown in Figure 2. Since the hydrate has a hexagonal structure, there are only two independent cell parameters (*a* and *c*) to be determined. Five Bragg reflections were used in the evaluation of the cell parameters. These peaks are the [212], [220], [310], [113] and [203] for HME hydrate and [212], [220], [113], [221] and [203] for DME hydrate. Occasionally, more peaks can be identified in the powder pattern.

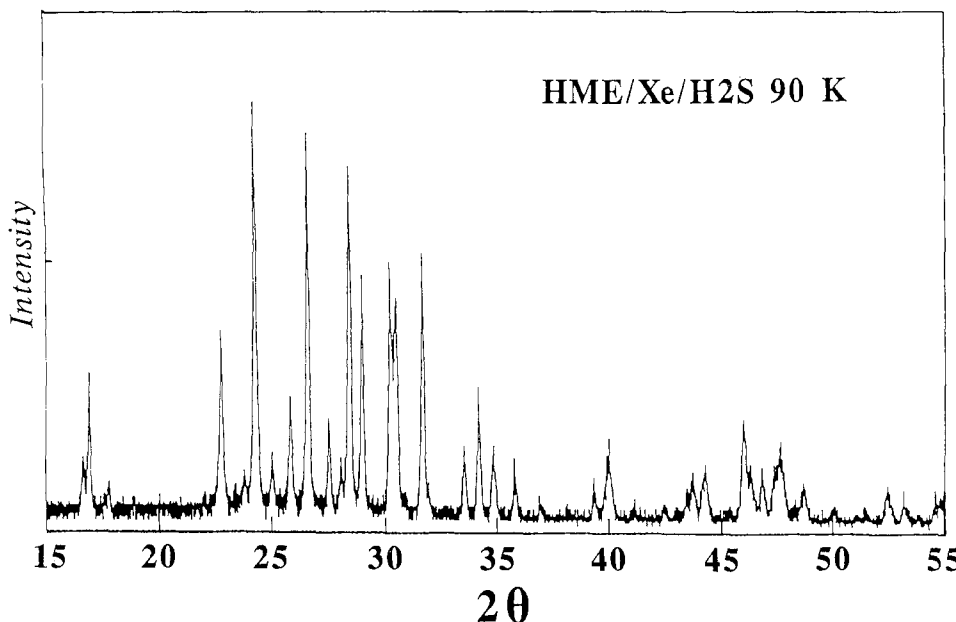


Fig. 1. X-ray diffraction pattern for HME hydrate at 90 K from 15 to 55°.

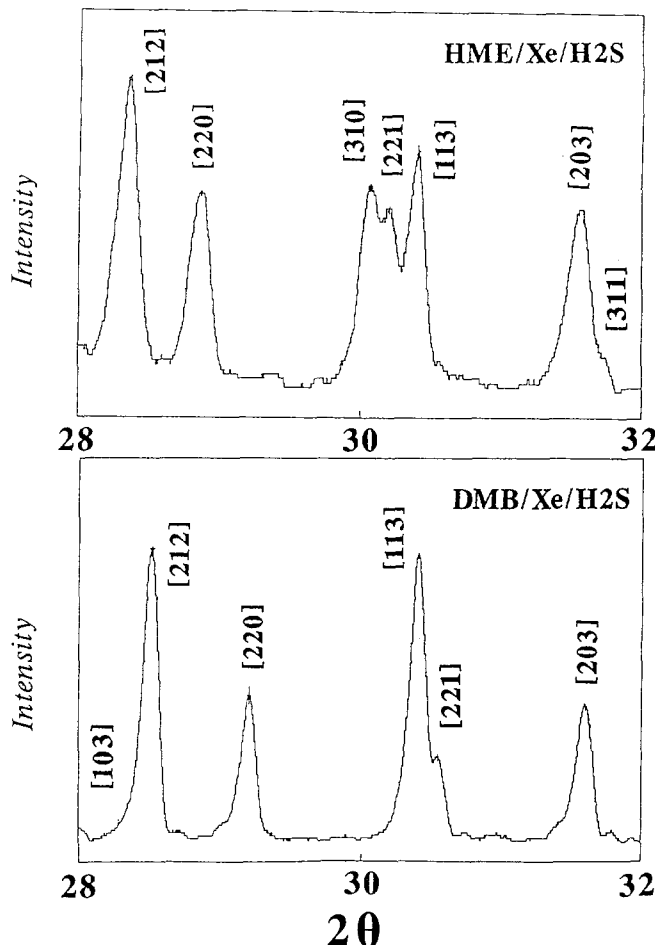


Fig. 2. X-ray diffraction pattern for HME hydrate (top) and DME hydrate (bottom) at 192.5 K in the region 28 to 32°.

However, they are not included in the least-squares refinement as these peaks are not well resolved and their positions cannot be located precisely at some temperatures. In passing, it is interesting to note that the HME hydrate is stable up to 230 K, the highest temperature studied here, while the DME hydrate started to decompose at about 205 K and converted completely into ice at about 230 K. The higher stability of the HME hydrate relative to DME hydrate is undoubtedly due to a lower vapour pressure of HME which is a solid at room temperature.

### 3. Results and Discussion

The unit cell parameters for HME and DMB hydrates as a function of temperature are depicted in Figure 3. The data points are somewhat scattered as only a limited number of low angle reflections were used in the evaluation of the cell parameters.

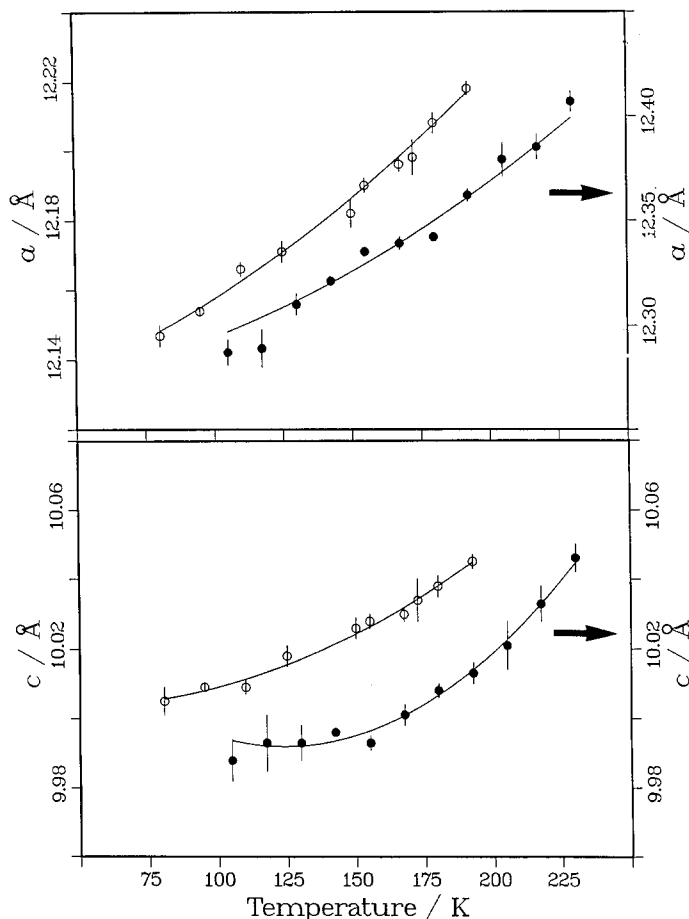


Fig. 3. Unit cell parameters for HME hydrate ( $\circ$ , left ordinate scale) and DMB hydrate ( $\bullet$ , right ordinate scale); (top)  $a$  axis and (bottom)  $c$  axis.

The scattering is more significant in the data for the  $c$  axis of HME hydrate at temperatures lower than 150 K. However, within the limits of accuracy of our measurements, we can make the following observations. The length of the  $a$  axis in HME hydrate is longer than that in DMB but the reverse is true for the  $c$  axis. The thermal expansions of the hydrates are anisotropic – the expansion along the crystallographic  $c$  axis is always smaller than that along the  $a$  axis. Over the temperature range studied here, the increase in the  $a$  and  $c$  axis in HME hydrate is 0.7% and 0.3%, respectively; for the DMB hydrate the increase is 0.5% and 0.4% respectively. In comparison, the increase in the unit cell sizes of both structure I hydrate of ethylene oxide (EO) and structure II hydrate of tetrahydrofuran (THF) is about 0.6% in the same temperature range.

The experimental data have been fitted with quadratic functions. The results are presented in Figure 3. The derived coefficients and standard deviation ( $\sigma$ ) of the fit for HME hydrate from 100–230 K are,

$$a(T)\text{\AA} = 12.268 + 0.697 \times 10^{-3}(T - 80)(\text{K}^{-1}) + 0.133 \times 10^{-5}(T - 80)^2(\text{K}^{-2}) \quad (1)$$

$$\sigma = 0.0051 \text{\AA}$$

$$c(T)\text{\AA} = 9.997 - 0.332 \times 10^{-3}(T - 80)(\text{K}^{-1}) + 0.430 \times 10^{-5}(T - 80)^2(\text{K}^{-2}) \quad (2)$$

$$\sigma = 0.0023 \text{\AA}$$

and for DME hydrate from 80–200 K,

$$a(T)\text{\AA} = 12.149 + 0.322 \times 10^{-3}(T - 80)(\text{K}^{-1}) + 0.238 \times 10^{-5}(T - 80)^2(\text{K}^{-2}) \quad (3)$$

$$\sigma = 0.0042 \text{\AA}$$

$$c(T)\text{\AA} = 10.006 + 0.122 \times 10^{-3}(T - 80)(\text{K}^{-1}) + 0.195 \times 10^{-5}(T - 80)^2(\text{K}^{-2}) \quad (4)$$

$$\sigma = 0.0019 \text{\AA}$$

One of the important properties that distinguish clathrate hydrates from ice is the thermal expansivity [21]. At low temperature, the thermal expansivities of the clathrate hydrates of ethylene oxide (structure I) [16] and tetrahydrofuran (structure II) [22] are found to be greater than ice; however, the difference becomes smaller when the temperatures are close to the melting points. The coefficient of linear expansion can be obtained by differentiating Equations 1–4. In Table I the thermal expansivities of the structure H hydrates at 150 and 200 K are compared with those of the cubic hydrates [16, 22] and ice [23, 24]. The thermal expansion of the *c* axis ( $\alpha_c = c^{-1} dc/dT$ ) is consistently *lower* than the *a* axis ( $\alpha_a = a^{-1} da/dT$ ) in the structure H hydrates. This observation is in contrast to ice  $I_h$  where the expansivities are almost identical for both axis [23, 24]. It would appear that the presence of guest molecules in the hydrate structure may induce an *anisotropy* in the thermal expansion of the water lattice. For DME hydrate, the thermal expansivity of the *a* axis is comparable to that of the EO hydrate [16] but is slightly larger than that of the THF hydrate [22]. In contrast, the thermal expansivity of the *a* axis in HME hydrate is larger than that in DME hydrate. Similar observation was also noted for the *c* axis. A more judicious way of comparing the expansion of crystals with different structures is to calculate the cubical expansion coefficients ( $\beta$ ). The coefficients of cubical expansion are given in the last column of Table I. It is

Table I. Coefficients of linear ( $\alpha$ ) and cubical ( $\beta$ ) expansion ( $\times 10^6$ ) for hydrates and ice

Hydrate	T(K)	$\alpha_a$	$\alpha_c$	$\beta$
HME	150	60	24	144
	200	78	71	227
DMB	150	54	40	148
	200	67	59	193
EO	150	56		147
	200	77		231
THF	150	42		126
	200	52		156
Ice $I_h$	150	28	25	81
	200	56	57	169

obvious that there is no discernible difference in the volume expansion among the hydrates considering the uncertainty associated with the derivatives evaluated from Equations 1–4. On the other hand, the data in Table I show that at 150 K the volume expansivities of all the hydrates are larger than that of ice. Moreover, the differences get smaller at 200 K. This observation, of course, is in accord with the conclusion reached in previous studies [16, 22].

In an earlier paper [16] it was demonstrated, through theoretical molecular dynamics calculations, that the relatively large thermal expansion in clathrate hydrates is mainly due to a unique role played by the guest. The collision of the guest with the cage wall through the localized vibrations [25] exerts an internal pressure that adds onto the expansion of the host lattice. It was shown [16] that a simple model based on the kinetic theory of gases is able to account for the volume expansion from the hypothetical empty hydrate to the enclathrated hydrate. The structural variation in the water lattices between hydrates and ice has little contribution to the difference in the thermal expansions. A similar explanation can be offered to rationalize the observations presented here. From NMR study [11], we found that xenon atoms can occupy the small cages in the structure H hydrates. Since the internal pressure of the crystal must be in equilibrium, only one type of cage will be considered. For instance, the pressure generated by xenon in the pseudospherical  $5^{12}$  cage, which is common to both structure I and II hydrates, will be similar to that of structure I xenon hydrate. Consequently, the volume expansion induced by such internal pressure should also be the same providing that the compressibilities (or bulk moduli) of the host lattices are comparable [26, 27]. This explains the near uniform volume expansion within the hydrates at the same temperature.

A larger thermal expansivity of the structure H hydrates as compared with ice indicates a stronger anharmonic crystal potential. Since the thermal resistivity of a crystal is a consequence of the scattering of thermal phonons by the anharmonic part of the interaction potential, we anticipate that the thermal conductivity of the structure H hydrate will also be lower than that of ice. Lower thermal conductivity has been observed for the cubic structure I and II [28, 29] hydrates. Similar information is not yet available for the structure H hydrate.

#### 4. Summary

In this preliminary study, it was found that the cubic expansion of the structure H hydrates of hexamethylethane (HME) and 2,2-dimethylbutane are comparable to those of the cubic structure I and II hydrates. An anisotropy in the thermal expansion of the two independent crystallographic *a* and *c* axes was also observed. The thermal expansivities of the two hydrates are broadly similar at temperatures higher than 150 K. At lower temperature, the thermal expansion of HME hydrate appears to be smaller than that in the DME hydrate. However, as mentioned earlier, the accuracy of the low temperature data is rather limited; more precise measurements and extension to lower temperature are needed in order to substantiate this observation.

This paper is dedicated to the memory of the late Dr D. W. Davidson who introduced the author to the fascinating field of clathrate hydrate research. His intellectual inspiration will always be remembered.

## Acknowledgements

The author wishes to thank Drs J. A. Ripmeester and C. I. Ratcliffe for providing the clathrate hydrate samples used in the present study.

## References

1. D. W. Davidson: in *Water – A Comprehensive Treatise*, Volume 2, ed. F. Franks, Plenum Press, New York, 1973.
2. G. A. Jeffrey: in *Inclusion Compounds*, Volume 1, eds. J. L. Atwood, J. E. D. Davies, and D. D. MacNicol, Academic Press, London, 1984.
3. M. von Stackelberg and H. R. Müller: *Z. Elektrochem.* **58**, 25 (1954).
4. M. von Stackelberg: *Naturwiss.* **36**, 327 (1949).
5. M. von Stackelberg and H. R. Müller: *J. Chem. Phys.* **19**, 1319 (1951).
6. G. D. Holder and D. J. Manganillo: *Chem. Eng. Sci.* **37**, 9 (1982).
7. D. W. Davidson, Y. P. Handa, C. I. Ratcliffe, J. S. Tse, and B. M. Powell: *Nature* **311**, 142 (1984).
8. J. S. Tse, Y. P. Handa, C. I. Ratcliffe, and B. M. Powell: *J. Incl. Phenom.* **4**, 235 (1986).
9. D. W. Davidson, Y. P. Handa, S. R. Gough, C. I. Ratcliffe, J. A. Ripmeester, and J. S. Tse: *J. de Physique (Paris)* **C1**, 537 (1987).
10. D. W. Davidson, M. A. Desando, Y. P. Handa, S. R. Gough, C. I. Ratcliffe, J. A. Ripmeester and J. S. Tse: *J. Incl. Phenom.* **5**, 219 (1987).
11. J. A. Ripmeester, J. S. Tse, C. I. Ratcliffe, and B. M. Powell: *Nature* **352**, 135 (1987).
12. H. Gies and H. Gerke: *Z. Kristallogr., Kristallgeom.* **166**, 11 (1984).
13. D. W. Davidson, Y. P. Handa, S. R. Gough, C. I. Ratcliffe, J. A. Ripmeester, J. S. Tse, and W. F. Lawson: *Geochim. Cosmochim. Acta* **50**, 619 (1986).
14. D. B. Glew and N. S. Rath: *J. Chem. Phys.* **44**, 1710 (1966).
15. G. H. Cady: *J. Phys. Chem.* **87**, 4437 (1983).
16. J. S. Tse, W. R. McKinnon, and M. Marchi: *J. Phys. Chem.* **91**, 4188 (1987).
17. D. W. Davidson, Y. P. Handa, C. I. Ratcliffe, J. A. Ripmeester, J. S. Tse, J. R. Dahn, F. L. Lee, and L. D. Calvert: *Mol. Cryst. Liq. Cryst.* **141**, 141 (1986).
18. E. J. Sonneveld and J. W. Visser: *J. Appl. Cryst.* **8**, 1 (1975).
19. J. Lacelle, A. Zagofsky, and S. Perlman: *J. Appl. Cryst.* **8**, 499 (1975).
20. G. Platbrood: *J. Appl. Cryst.* **16**, 24 (1983).
21. D. F. Sargent and L. D. Calvert: *J. Phys. Chem.* **70**, 2689 (1966).
22. J. S. Tse: *J. Physique (Paris)* **C1**, 543 (1987).
23. S. LaPlaca and B. Post: *Acta Crystallogr.* **13**, 503 (1963).
24. R. Brill and A. Tippe: *Acta Crystallogr.* **23**, 343 (1967).
25. J. S. Tse, M. L. Klein, and I. R. McDonald: *J. Chem. Phys.* **89**, 3103 (1985).
26. H. Kiefte, M. J. Clouter, and R. E. Gagnon: *J. Phys. Chem.* **89**, 3103 (1985).
27. P. Gammon, H. Kiefte, and M. J. Clouter: *J. Phys. Chem.* **87**, 4025 (1983).
28. R. G. Ross, P. Andersson, and G. Backström: *Nature* **290**, 322 (1981).
29. J. S. Tse and M. A. White: *J. Phys. Chem.* **92**, 5006 (1988).